

High Efficiency Detection of Argon Scintillation Light of 128nm Using LAAPDs

Rico Chandrasekharan^{*†‡}, Andreas Knecht^{*}, Marcello Messina^{*}, Christian Regenfus[†], and André Rubbia^{*}

^{*} ETH Zürich, Institut für Teilchenphysik, CH-8093 Zürich, Switzerland

[†] University of Zürich, Physik Institut, Winterthurerstr. 190, CH-8057 Zürich, Switzerland

[‡] Email: rico.chandrasekharan@cern.ch, Telephone: ++41 22 767 1474, Fax: ++41 22 767 1411

Abstract—The possibility of efficient collection and detection of vacuum ultraviolet light as emitted by argon, krypton, and xenon gas is studied. Absolute quantum efficiencies of large area avalanche photodiodes (LAAPDs) are derived at these wavelengths. VUV light of wavelengths down to the 128nm of Ar emission is shown to be detectable with silicon avalanche photodiodes at quantum efficiencies above 42%. Flexible Mylar foil overcoated with Al+MgF₂ is measured to have a specular reflectivity of $\sim 91\%$ at argon emission wavelength. Low-pressure argon gas is shown to emit significant amounts of non-UV radiation. The average energy expenditure for the creation of non-UV photons in argon gas at this pressure is measured to be below 378 eV.

Index Terms—VUV light, APD, argon scintillation, quantum efficiency, Al+MgF₂.

I. INTRODUCTION

THE ArDM detector currently under construction is a WIMP detector prototype based on argon bi-phase technology, see [1]. In this detector, the detection of the 128 nm argon scintillation light as well as a localized charge readout allow discrimination against gamma/beta backgrounds. A major goal of the project is the proof of scalability of such technology to large target masses. ArDM is aiming to be among the first large direct dark matter detectors, with a target mass of the order of one metric ton.

In the last two years extensive R&D has been conducted towards the achievement of this goal. This included investigation of the possibility to reflect VUV photons on Al coated mylar foils as a means of light collection. For light detection purposes, the feasibility of using large area avalanche photodiodes (LAAPD) for light read-out was analyzed. This talk presents the results of the measurement of the quantum efficiency of such devices.

Noble gases are known to provide scintillation light with high yield, up to about 50 photons per keV electron equivalent. Detection of this light proves fundamental in many applications in which noble gas is used as medium. Difficulties arise from the fact that noble gas emission is peaked in the vacuum ultraviolet (VUV) range. To detect such light, wavelength shifter-coated photomultiplier tubes (PMTs) have often been used, resulting in a low global quantum efficiency, typically $\leq 10\%$. There is interest in knowing if LAAPDs could be

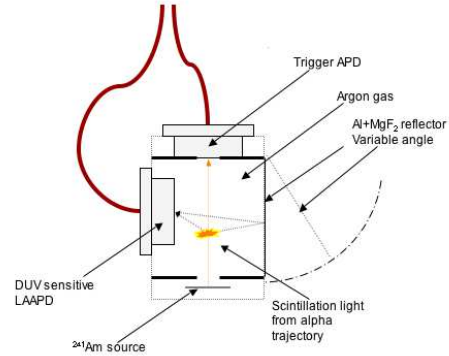


Fig. 1

ALPHA PARTICLES PASS FROM THE SOURCE TO AN APD SERVING AS TRIGGER. A LATERALLY MOUNTED APD MEASURES THE SCINTILLATION LIGHT EMITTED ALONG THE TRAJECTORY. A VUV REFLECTING MIRROR MAY BE PLACED AT A DESIRED ANGLE, ENHANCING THE SIGNAL.

a viable alternative, in particular in applications where the radiopurity is a concern.

The presented results show that it is in principle possible both to collect VUV light using mirrors, as well as to detect gas scintillation from Kr, Xe and Ar with APDs at a quantum efficiency significantly higher than with PMTs. The issues related to the signal to noise of APDs, to the parallel operation of a large number of APDs to increase the sensitive area, and the mechanical problems at potential cryogenic temperatures are not addressed in this paper.

II. EXPERIMENTAL SETUP

In our experimental setup (See Figure 1), we detect argon gas scintillation light with an LAAPD mounted on an axis perpendicular to the trajectory of alpha particles. The alpha particles pass from the open ²⁴¹Am source to a second APD employed as a trigger. The setup for quantum efficiency measurements is described in more detail in [2].

The APDs are Advanced Photonix LAAPDs with an active diameter of 16mm [3]. For scintillation light detection a

windowless, 'DUV-enhanced' device was used primarily, cross-checked against a windowless 'Red/IR-enhanced' device.

At the gas pressures used, the decay time of the argon scintillation signal is of the order of several microseconds [8]. Long shaping times allow full integration of the complete signal.

Measuring the current flowing through the APD allows the gain to be monitored according to the method described in [4], where a LED situated inside the dewar serves as a continuous light source.

For the reflectivity measurements presented in Section V, a VUV reflecting mirror (also shown in Figure 1) may be placed at a desired angle, enhancing the signal. Via a mechanical feed-through, the mirror angle may be set to values between $\phi = 0$ and $\phi = 90$ degrees, where ϕ is defined as the angle between the mirror plane and the alpha trajectory. The setup for reflectivity measurements is described in more detail in [5].

III. SIMULATION OF PHOTON YIELD

The gases used in this work- Ar, Kr, and Xe- emit photons around 128nm, 150nm, and 175nm, respectively. The VUV photon production mechanism in argon and other noble gases is known, see for example [6] and citations therein/thereof. Accordingly, the average energy expenditure for the emission of a VUV scintillation photon in pure argon gas is $W_{\gamma}^{VUV} = 67.9$ eV. Similarly, for krypton and xenon, $W_{\gamma}^{VUV} = 61.2$ eV and 55.9 eV, respectively (See Appendix).

The α 's trajectory in our setup is well defined due to collimation. Given the gas temperature and pressure, the energy loss of the α along its trajectory can then be computed [7]. The number of VUV photons created and emitted into the solid angle subtended by the LAAPD can be simulated for an α following its trajectory. In the following, this number is referred to as N_{γ}^{sim} .

For the reflectivity measurements of Section V, the simulation additionally computes the number of photons reaching the APD indirectly through specular reflection by the mirror placed at a variable angle ϕ . This value is referred to as $N_{\gamma}^{sim}(\phi)$.

The simulated ratio of indirect i.e. reflected to direct light is

$$N_{\gamma}^{sim}(\phi)/N_{\gamma}^{sim}. \quad (1)$$

This can then be compared to the measured values.

IV. QUANTUM EFFICIENCY MEASUREMENT

A number of measurements were performed in argon, krypton, and xenon gas. The gas pressures were chosen to ensure the alphas depositing sufficient energy in the trigger APD.

The external quantum efficiency of APDs, from now on referred to as quantum efficiency, is defined as the number of primary electron-hole pairs produced per incident photon. The quantum efficiency $\epsilon_Q(\lambda)$ is a function of the wavelength of the incident light.

The quantum efficiency and APD gain G relate to the charge signal Q_S via

$$G \cdot e \cdot \epsilon_Q(\lambda) \cdot N_{\gamma}^{sim} = Q_S \quad (2)$$

TABLE I

THE GAIN-INDEPENDENT SIGNAL NORMALIZED TO THE EXPECTED NUMBER OF VUV PHOTONS IN ARGON. MEASUREMENTS PERFORMED USING 'DUV-ENHANCED' LAAPD. ALL DATA WAS ACQUIRED USING A SHAPING TIME OF 10 μ S. THE LAST LINE GIVES THE AVERAGE VALUE OF THE MEASUREMENTS.

p_{Ar} (atm)	T_{Ar} (°K)	Gain	Q_S (fC)	N_{γ}^{sim}	$\frac{Q_S}{e \cdot N_{\gamma}^{sim} \cdot G}$
0.830	282.5	69 \pm 5	25.6 \pm 1.0	3238	0.72 \pm 0.05
0.777	281.5	67 \pm 5	24.5 \pm 0.9	2956	0.77 \pm 0.06
0.750	281.4	57 \pm 4	17.7 \pm 0.7	2815	0.69 \pm 0.05
0.719	281.3	57 \pm 4	16.7 \pm 0.5	2659	0.69 \pm 0.05
0.678	281.2	53 \pm 4	15.5 \pm 0.7	2461	0.74 \pm 0.06
Ar	DUV-enh				0.72 \pm 0.06

TABLE II

THE GAIN-INDEPENDENT SIGNAL NORMALIZED TO THE EXPECTED NUMBER OF VUV PHOTONS IN KRYPTON (SEE TEXT). MEASUREMENTS PERFORMED USING 'DUV-ENHANCED' LAAPD AT 10 μ S SHAPING TIME. THE LAST LINE GIVES THE AVERAGE VALUE OF THE MEASUREMENTS.

p_{Kr} (atm)	T_{Kr} (°K)	Gain	Q_S (fC)	N_{γ}^{sim}	$\frac{Q_S}{e \cdot N_{\gamma}^{sim} \cdot G}$
0.629	285.0	26.1 \pm 1.8	15.6 \pm 0.6	3844	0.97 \pm 0.08
0.600	284.4	28.1 \pm 2.1	15.8 \pm 0.6	3613	0.97 \pm 0.08
0.573	284.0	25.1 \pm 1.6	15.5 \pm 0.6	3402	1.13 \pm 0.08
0.551	283.9	25.3 \pm 1.6	14.3 \pm 0.5	3246	1.08 \pm 0.08
0.514	283.9	27.3 \pm 1.9	13.8 \pm 0.5	2960	1.06 \pm 0.08
Kr	DUV-enh				1.04 \pm 0.08

where e is just the elementary charge. By comparing N_{γ}^{sim} with the measured charge signal, the quantum efficiency can be stated, see Tables I,II,&III.

In the gas phase there is evidence that noble gas scintillation light contains non-UV components. Additional measurements were performed to subtract contributions from possible non-UV components of argon scintillation light. This was done by employing a 'Red/IR-enhanced' LAAPD of the same make. The device has a 150nm thick SiO_2 anti-reflective coating, rendering it largely insensitive to VUV light. In a further measurement, a 0.1 mm thick UV-attenuator of plastic foil was mounted in front of the 'Red/IR-enhanced' LAAPD, see Table IV.

A quantitative estimate of the non-UV emission components of argon emission was achieved. An upper limit for the average amount of energy needed to produce a non-UV photon in argon gas around at near ambient pressure is found to be

$$W_{\gamma}^{IR} \leq 378 \text{ eV}. \quad (3)$$

The quantum efficiencies measured in Tables I,II,&III need to be corrected for the non-UV components (See Appendix). This was done in a conservative way, leading to a lower limit of 42% for the true quantum efficiency 128 nm. The non-UV components were only measured in argon, see Figure 2.

TABLE III

THE GAIN-INDEPENDENT SIGNAL NORMALIZED TO THE EXPECTED NUMBER OF VUV PHOTONS IN XENON (SEE TEXT). MEASUREMENTS PERFORMED USING 'DUV-ENHANCED' LAAPD AT $10\mu\text{s}$ SHAPING TIME. THE LAST LINE GIVES THE AVERAGE VALUE OF THE MEASUREMENTS.

p_{Xe} (atm)	T_{Xe} (°K)	Gain	Q_s (fC)	N_γ^{sim}	$\frac{Q_s}{e \cdot N_\gamma^{sim} \cdot G}$
0.430	286.4	26.1 ± 1.8	20.6 ± 0.8	3786	1.29 ± 0.10
0.407	285.3	25.6 ± 1.7	19.1 ± 0.7	3551	1.31 ± 0.10
0.379	284.9	25.6 ± 1.7	18.0 ± 0.7	3256	1.35 ± 0.10
0.372	286.0	24.6 ± 1.6	16.0 ± 0.6	3163	1.28 ± 0.10
Xe	DUV-enh				1.3 ± 0.1

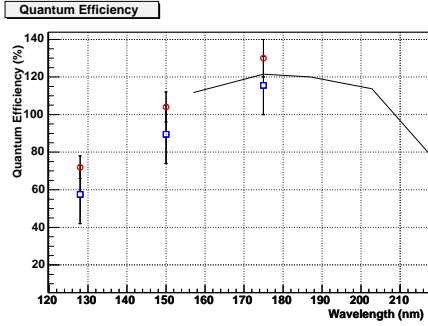


Fig. 2

THE QUANTUM EFFICIENCY OF THE 'DUV-ENHANCED' LAAPD: THE CONTINUOUS CURVE DEPICTS THE VALUES GIVEN BY THE MANUFACTURER [3]. THE CIRCLES REPRESENT THE VALUES MEASURED AT ARGON, KRYPTON, AND XENON EMISSION WAVELENGTHS. THE SQUARE MARKERS INCLUDE THE CORRECTION FOR NON-UV COMPONENTS AS MEASURED IN ARGON.

TABLE IV

MEASUREMENTS PERFORMED IN ARGON WITH THE 'RED/IR-ENHANCED' LAAPD. THE MIDDLE LINE GIVES THE AVERAGE VALUE OF THE TOP THREE MEASUREMENT SERIES. THE LOWER HALF OF THE TABLE SHOWS RESULTS OF MEASUREMENTS PERFORMED WITH A UV ABSORBING FOIL IN FRONT OF THE 'RED/IR-ENHANCED' LAAPD (SEE TEXT). THE AVERAGE VALUE OF THESE MEASUREMENT SERIES IS GIVEN IN THE LAST LINE.

p_{Ar} (atm)	T_{Ar} (°K)	Gain	Q_s (fC)	N_γ^{sim}	$\frac{Q_s}{e \cdot N_\gamma^{sim} \cdot G}$
0.835	275.9	79.9	10.2	3388	0.23
0.820	276.7	77.6	9.39	3281	0.23
0.806	276.7	80.0	9.98	3197	0.24
Ar	Red/IR-enh				0.233
0.862	278.7	90.4	7.2	3505	0.14
0.847	279.2	159.9	13.6	3400	0.16
0.830	279.1	168.5	14.5	3303	0.16
Ar	Red/IR+Filter				0.153

TABLE V

RESULTS OF THE QUANTUM EFFICIENCY MEASUREMENTS COMPARED TO THE MANUFACTURER'S DATA WHERE AVAILABLE.

	λ (nm)	QE \geq	QE \leq	QE manufacturer
Ar	128	42%	73%	n.a.
Kr	150	74%	113%	112% @ 157nm
Xe	175	100%	140%	123%

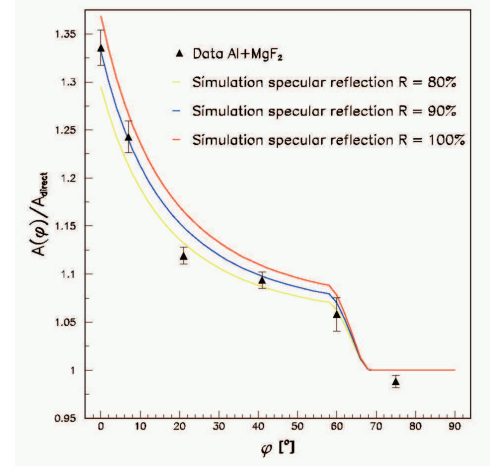


Fig. 3

THE ANGULAR DEPENDENCE OF THE MEASURED SPECULAR REFLECTIVITY OF THE AL+MgF₂ FOIL IS IN GOOD AGREEMENT WITH SIMULATION FOR A SPECULAR REFLECTIVITY OF 90% AT 128 NM.

The obtained values agree well with the data given by the manufacturer for xenon and krypton emission wavelengths, see Figure 2.

V. REFLECTIVITY MEASUREMENT

In our search for efficient light collection techniques, we included a variable angle VUV reflector in our setup, see Figure 1. The reflector consists of a $125\ \mu\text{m}$ Mylar foil overcoated with 85 nm aluminum and 25 nm MgF₂ to prevent aluminum oxidation.

The aluminum reflector evaporated on flexible mylar foil is overcoated with a 20nm MgF₂ film to prevent oxidation.

Reflectivity measurements were performed by measuring the APD signal height at different mirror angles. Each such measurement was normalized by the signal height at $\phi = 90$ degrees where no reflected light contributes to the signal. These ratios were compared to the simulated ratios $N_\gamma^{sim}(\phi)/N_\gamma^{sim}$, see Figure 3.

Our measured values are consistent with those of [10], stating a specular reflectivity of $\sim 90\%$ at 128 nm for $Al + MgF_2$ on a glass substrate (See Figure 4).

VI. CONCLUSION

Vacuum ultraviolet light can be detected by LAAPDs with improved quantum efficiency compared to other means such

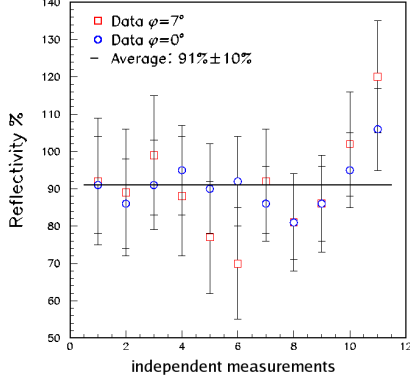


Fig. 4

THE MEASURED SPECULAR REFLECTIVITY OF THE AL+MGF₂ FOIL IS IN GOOD AGREEMENT WITH THE LITERATURE VALUE OF 90% AT 128 NM.

as wavelength-shifter coated photomultipliers. Figure 2 summarizes the obtained results for argon, krypton, and xenon. Our measurements are consistent with the manufacturer's data where it is available. The non-UV correction was only measured for argon. For xenon and krypton this correction is of illustrative nature only. Since light quenching by remnant impurities in the gas or by remnant air/water in the volume was not considered, the lower limit of $\epsilon_q^{VUV}(128nm) \geq 42\%$ is strict while the upper limit is not.

At room temperature, single photon counting was not achieved with the device used. Preliminary tests suggest that even at low temperatures the noise associated with this particular device's high capacitance makes single photon detection difficult. This renders it impractical for the use in ArDM. We do not exclude photon counting possibility with smaller devices of lower capacitance from the same manufacturer, operated at LAr temperatures.

The principle of VUV light collection by means of reflecting foils has been shown to work. The fact that the foils are flexible makes them a very handy tool for all liquid noble gas experiments. Applications include the construction of Winston cones or other light concentrators.

APPENDIX

COMPUTATION OF W_γ^{VUV} IN NOBLE GASES

The average energy expended per ion pair W_g^{ion} can be related to the ionization potential I [6]

$$\frac{W_g^{ion}}{I} = \frac{E_i}{I} + \left(\frac{E_{ex}}{I}\right) \left(\frac{N_{ex}}{N_i}\right) + \frac{\epsilon}{I}, \quad (4)$$

where N_i is the number of ions produced at an average energy expenditure of E_i , N_{ex} is the number of excited atoms produced at an average expenditure of E_{ex} , and ϵ is the average kinetic energy of escape electrons.

Equation 4 is energy dependent in all four terms, however, for $E \gg I$ this dependence is weak. For α -particles in argon, $W_g^{ion} = 26.5 \pm 0.5$ eV at energies $E_\alpha \geq 1$ MeV. For $E_\alpha = 0.1$ MeV, the value is only somewhat higher at $W_g^{ion} = 27.5 \pm 1.0$ eV, increasing further as the kinetic energy is reduced. Our measurements were performed in a pressure range where the scintillation is brought forth by α particles with at least 0.5 MeV kinetic energy.

Assuming no ionization contribution to UV scintillation light, justified at the low pressures used in this work [11], the average energy expenditure per photon is

$$W_\gamma^{VUV} = \left(\frac{N_i}{N_{ex}}\right) \cdot E_i + E_{ex} + \left(\frac{N_i}{N_{ex}}\right) \cdot \epsilon \quad (5)$$

electron volts. Substituting Equation 4 in Equation 5 gives

$$W_\gamma^{VUV} = W_g^{ion} \cdot \frac{N_i}{N_{ex}} \quad (6)$$

The values of W_g^{ion} and $\frac{N_{ex}}{N_i}$ can be obtained from [9], giving $W_\gamma^{VUV} = 67.9$ eV, 61.2 eV, and 55.9 eV for Ar, Kr, and Xe, respectively.

ESTIMATION OF W_γ^{IR}

Using the data listed in Table IV, we can give a strict lower limit for the branching ratio N^{IR}/N_γ^{sim} of the emission of non-UV photons in argon. The number of non-UV photons impinging on the 'Red/IR-enhanced' LAAPD relates to the detected charge signal in linear dependence of gain and quantum efficiency:

$$N^{IR} = \frac{Q_S}{e \cdot \epsilon_Q(\lambda) \cdot G} \quad (7)$$

The expression is minimized by the maximum quantum efficiency of the Red/IR-enhanced APD, giving the expression

$$\left(\frac{Q_S}{e \cdot N_\gamma^{sim} \cdot G}\right)_{Red/IR+Filter} \cdot \frac{1}{\max \epsilon_Q(\lambda)} = 0.18 \leq \frac{N^{IR}}{N_\gamma^{sim}}, \quad (8)$$

where

$$\max_{270 \leq \lambda \leq 1050} \epsilon_Q(\lambda) = 0.85 \quad (9)$$

was used.

By comparison with W_γ^{VUV} (See Equation 6), the obtained value can be translated into

$$W_\gamma^{IR} \leq 378 \text{ eV}, \quad (10)$$

a strict upper limit for the average amount of energy needed to produce a non-UV photon in argon gas around this pressure.

NON-UV CORRECTION FOR $\epsilon_Q(128nm)$

With the data in Table IV, the quantum efficiency of the 'DUV-enhanced' LAAPD for radiation at 128 nm can be calculated more precisely. In Equation 2, the measured charge signal Q_S (See Table I) is actually the sum

$$Q_S = eG(N_\gamma \epsilon_Q(128nm) + N^{IR}(\lambda) \epsilon_Q(\lambda)) \quad (11)$$

of the VUV contribution and of the non-UV contribution, both weighted with the quantum efficiency of the 'DUV-enhanced' APD at the respective wavelength. The equation can be rewritten as

$$\epsilon_Q^{uncorrected} = \frac{N_\gamma \epsilon_Q(128nm) + N^{IR}(\lambda) \epsilon_Q(\lambda)}{N_\gamma} \quad (12)$$

and

$$\epsilon_Q(128nm) = \epsilon_Q^{uncorrected} - \frac{N^{IR}(\lambda)}{N_\gamma} \cdot \epsilon_Q(\lambda). \quad (13)$$

The value of the ratio N^{IR}/N_γ^{sim} is contained in an interval given by the measurements in Table IV in a similar way as was done in Equation 8. Thus, a strict lower limit,

$$\epsilon_Q(128nm) \geq \left(\frac{Q_S}{e \cdot N_\gamma^{sim} \cdot G} \right)_{VUV} - \left(\frac{Q_S}{e \cdot N_\gamma^{sim} \cdot G} \right)_{IR} \cdot \max_\lambda \frac{\epsilon_q^{VUV}(\lambda)}{\epsilon_q^{IR}(\lambda)}$$

and, as an upper limit

$$\epsilon_Q(128nm) \leq \left(\frac{Q_S}{e \cdot N_\gamma^{sim} \cdot G} \right)_{VUV} - \left(\frac{Q_S}{e \cdot N_\gamma^{sim} \cdot G} \right)_{IR+Filter} \cdot \min_\lambda \frac{\epsilon_q^{VUV}(\lambda)}{\epsilon_q^{IR}(\lambda)}$$

can be given, superindices denoting which APD the quantum efficiency refers to, subindices labelling measurements from the right most column of Tables I and IV. In the above equations, the extrema of the ratio $\epsilon_Q^{VUV}(\lambda)/\epsilon_Q^{IR}(\lambda)$ of the quantum efficiencies of the two LAAPD types used can be obtained from the manufacturer's data sheet on an interval from 270nm to 1050nm.

This gives

$$0.42 \leq \epsilon_q^{VUV}(128nm) \leq 0.73 \quad (14)$$

where the upper limit is not rigorous as quenching effects due to gas impurities have not been accounted for.

If argon non-UV emission is centered around 940 nm as measured by [12], this would result in an in-between value of $\epsilon_Q^{VUV}(128nm) \approx 0.58$. Note that over a large region of the IR spectrum, the ratio of $\epsilon_Q^{VUV}/\epsilon_q^{IR}$ is relatively constant, making $\epsilon_Q^{VUV}(128nm)$ relatively insensitive to the exact wavelength of peak IR emission.

ACKNOWLEDGMENT

This work is presented on behalf of the ArDM group, consisting of scientists working for ETH Zürich and the University of Zürich in Switzerland, CIEMAT and the University of Granada in Spain, and the Soltan Institute Warsaw in Poland. We thank the Thin Film Workshop at CERN, in particular A. Braem, for providing the reflecting foils and useful discussions.

REFERENCES

- [1] A. Rubbia, *ArDM: A ton-scale liquid argon experiment for direct detection of dark matter in the universe*, Talk given at IXth International conference on Topics in Astroparticle and Underground Physics (TAUP05), Zaragoza (Spain), Sep. 2005. arXiv:hep-ph/0510320. See also <http://neutrino.ethz.ch/ArDM>
- [2] R. Chandrasekharan, M. Messina, and A. Rubbia, *Detection of noble gas scintillation light with large area avalanche photodiodes (LAAPDs)*, Nucl. Instr. and Methods in Phys. Res. A 546 (2005) 426-437. doi:10.1016/j.nima.2005.03.105
- [3] Advanced Photonix, Inc. See <http://www.advancedphotonix.com/>
- [4] A. Karar, Y. Musienko, and J. Ch. Vanel, *Characterization of avalanche photodiodes for calorimetry applications* Nucl. Instr. and Methods in Phys. Res. A 428 (1999) 413-431. doi:10.1016/S0168-9002(99)00177-1
- [5] A.Knecht, *Improvement of VUV Light Collection for a Future Dark Matter Detector*, Diploma Thesis ETH Zurich August 2005. Available at <http://neutrino.ethz.ch/diplomathesis.html>
- [6] M. Miyajima, T. Takahashi, S. Konno, T. Hamada, S. Kubota, H. Shibamura, and T. Doke, *Average energy expended per ion pair in liquid argon*, Phys. Rev. A 9,3 (1974) 1438.
- [7] M.J. Berger, J.S. Coursey, and M.A. Zucker *Stopping-Power and Range Tables for Electrons, Protons, and Helium Ions*, <http://physics.nist.gov/PhysRefData/Star/Text/contents.html>
- [8] P. Moerman, R. Boucique, and P. Mortier, *Pressure Dependent Decay of the Ultraviolet Continuum of Argon* Phys. Lett. A 49, 2 (1974) 179.
- [9] R. L. Platzman, *Total Ionization in Gases by High-Energy Particles: An Appraisal of Our Understanding*, Int. J. Appl. Radiat. and Isot. 10 (1961) 116. International Commission on Radiation Units and Measurements, *Average energy required to produce an ion pair*, ICRU Report 31, 1979.
- [10] A.P. Bradford, G. Hass, J. F. Osantowski, and A. R. Toft, *Preparation of Mirror Coatings for the Vacuum Ultraviolet in a 2-m Evaporator*, Applied Optics Vol. 8, No. 6 (1969) 1183 .
- [11] M. Suzuki, *Recombination Luminescence from Ionization Tracks Produced by Alpha Particles in High pressure Argon, Krypton and Xenon Gases*, Nucl. Instr. and Methods 215 (1983) 345-356. M.J. Carvalho and G. Klein, *Alpha-Particle Induced Scintillation in Dense Gaseous Argon: Emission Spectra and Temporal Behaviour of its Ionic Component*, Nucl. Instr. and Methods 178 (1980) 469-475.
- [12] G. Bressi, G. Carugno, E. Conti, D. Iannuzzi, A.T. Meneguzzo, *A first study of the infrared emission in argon excited by ionizing particles*, Phys. Lett. A 278 (2001) 280-285.